JOURNAL OF MATERIALS SCIENCE 30 (1995) 5065–5072

Stress–strain rate relations for high-temperature deformation of two-phase Al–Cu alloys

P. K. BAKSHI*, B. P. KASHYAP
Department of Metallurgical Engineering and Materials Science, Indian Institute of Technology, Bombay 400076, India

Al–Cu alloys containing 6, 11, 17, 24 and 33 wt % Cu, annealed for 0.5–100 h, were deformed by the differential strain-rate test technique over a strain-rate range of $\approx 4 \times 10^{-6}$ to $3 \times 10^{-2} s^{-1}$ at temperatures ranging from 460–540° C. Superplastic behaviour, with strain-rate sensitivity, $m \approx 0.5$, and activation energy, $Q = 171.5$ kJ mol^{-1}, is shown by the Al–24Cu and Al–33Cu alloys at lower strain rates and higher temperatures. All the alloys show $m \lesssim 0.20$ at higher strain rates, but the average activation energy for deformation of the Al–6Cu, Al–11Cu, and Al–17Cu alloys is evaluated to be 480.7 kJ mol^{-1}, in contrast to a lower value of 211 kJ mol^{-1} for the Al–24Cu and Al–33Cu alloys. Instead of grain size, the mean free path between θ particles is suggested to be a more appropriate microstructural parameter for the constitutive relationship for deformation of the Al–Cu alloys.

1. Introduction

During high-temperature deformation, the flow stress, σ, depends on strain rate, $\dot{\varepsilon}$, test temperature, T (K) and grain size, d, according to the relationship [1]

$$\dot{\varepsilon} = \frac{AD_0Eb}{kT}\left[\frac{b}{d}\right]^p\left[\frac{\sigma}{E}\right]^n \exp\left[-\frac{Q}{RT}\right] \quad (1)$$

where $D_0 \exp(-Q/RT)$ is the appropriate diffusion coefficient D, E is the Young's modulus, b is the Burgers vector, $n(=1/m)$ is the stress exponent which is equal to the inverse of the strain-rate sensitivity index, m, p is the grain-size exponent. A is the microstructural- and mechanism-dependent constant, and R, k have their usual meanings. The alloys with fine microstructures ($d < 10$ μm) can yield exceptionally large ductility, called superplasticity, under suitable test conditions [2]. During superplastic deformation, the parameters of Equation 1 are evaluated to be $n \approx 2.0$, $Q = Q_{gb}$, the activation energy for grain-boundary diffusion, and $p = 2$–3.

In the two-phase materials, however, often no distinction is made between the phases while relating to the flow behaviour; the average phase size is the only microstructural parameter employed in the constitutive relationship. However, Suery and Baudelet [3] have recently incorporated the volume fraction of the constituent phases in the constitutive relationship for superplastic deformation as

$$\dot{\varepsilon} \approx \left[\frac{1-\alpha}{\alpha}\right]^2 \frac{\sigma^2}{L_\beta^2} \exp\left[-\frac{Q}{kT}\right] \quad (2)$$

Here α is the volume fraction of α phase, L_β is the grain size of the β phase, and the other terms have the same meanings as in Equation 1.

In the Al–Cu system, the eutectic alloy has been extensively investigated [5–15] for its superplastic behaviour but there appear only few such or related studies [11, 16, 17] on the hypoeutectic composition. As the copper content in the Al–Cu alloy is increased, the volume fraction of θ phase, which is much stronger than the κ phase [18], increases. This results in a reduction in the mean grain size. Thus, in the two-phase Al–Cu alloys of varying compositions, the deformation behaviour should be a function of grain size and phase proportion. As no such study has been reported in the Al–Cu alloys, it was the aim of this investigation to examine the influence of grain size and κ/θ phase proportion on high-temperature flow behaviour.

2. Experimental procedure

Five Al–Cu alloys with compositions (wt % throughout) given in Table I were prepared into 1.8 mm thick sheets by melting and rolling as described earlier [19].

Tensile specimens of gauge length 25 mm and gauge width 6 mm were machined, and then annealed for 0.5–100 h at 535° C to obtain various grain sizes. Metallographic specimens were prepared and the sizes of the individual grains and phases were measured as described earlier [19]. The grain sizes for evaluating grain growth due to deformation were measured by the mean intercept length method, with no distinction being made between the κ and θ phases. More than 300 grains were considered for each size data reported here and the errors in the average grain sizes were within ± 10% at 95% confidence level.

*Present address: Department of Metallurgy, Government Engineering College, Raipur 492010, India.

TABLE I Chemical composition (wt %) of the Al–Cu alloys

Alloy	Designation	Cu	Fe	Si	Zn	Ni	Mn	Mg	Pb	Al
1	Al–6Cu	5.0	0.13	0.15	0.01	0.012	0.002	0.004	0.005	Bal.
2	Al–11Cu	11.0	0.12	0.15	0.006	0.012	0.002	0.023	0.005	Bal.
3	Al–17Cu	17.03	0.11	0.152	0.006	0.012	0.0011	0.0033	0.005	Bal.
4	Al–24Cu	24.38	0.29	0.15	0.023	0.012	0.006	0.003	0.005	Bal.
5	Al–33Cu	33.39	0.09	0.048	0.006	0.012	0.0018	0.0024	0.005	Bal.

TABLE II Grain sizes of κ-phase, d_κ, and θ phase, d_θ, in the Al–Cu alloys of different compositions upon annealing at 535 °C

Annealing time (h)	Al–6Cu		Al–11Cu		Al–17Cu		Al–24Cu		Al–33Cu	
	d_κ (μm)	d_θ (μm)	d_κ (μm)	d_θ (μm)	d_κ (μm)	d_θ (μm)	d_κ (μm)	d_θ (μm)	d_κ (μm)	d_θ (μm)
0.5	34.1	3.1	11.9	4.9	9.6	4.7	7.1	5.3	7.4	6.4
4.0	37.7	3.8	11.9	6.1	9.5	5.9	6.3	5.8	6.9	6.6
10.0	41.9	4.3	13.6	5.8	9.1	6.4	7.1	7.0	7.3	9.9
100.0	55.3	4.0	17.8	7.1	11.3	6.8	12.4	8.8	9.3	8.8

TABLE III Sizes of κ-phase, p_κ, and θ-phase, p_θ, in the Al–Cu alloys of different compositions upon annealing at 535 °C

Annealing time (h)	Al–6Cu		Al–11Cu		Al–17Cu		Al–24Cu		Al–33Cu	
	p_κ (μm)	p_θ (μm)	p_κ (μm)	p_θ (μm)	p_κ (μm)	p_θ (μm)	p_κ (μm)	p_θ (μm)	p_κ (μm)	p_θ (μm)
0.5	61.2	4.8	22.0	6.2	17.9	7.1	13.1	10.7	10.6	13.8
4.0	128.0	5.2	21.2	7.3	15.3	8.5	13.0	9.4	11.1	13.2
10.0	51.4	5.4	22.2	6.6	16.7	9.0	14.1	11.2	12.1	13.6
100.0	109.3	5.0	26.5	7.6	19.8	9.5	18.4	16.7	18.1	17.3

TABLE IV Mean free path, Λ, between θ particles in the alloys of different compositions at a test temperature of 535 °C upon annealing for various lengths of time

Annealing time (h)	Λ (μm)				
	Al–6Cu	Al–11Cu	Al–17Cu	Al–24Cu	Al–33Cu
0.5	636.8	29.7	14.7	10.9	6.6
4.0	689.9	35.0	17.7	9.6	6.3
10.0	716.4	31.7	18.7	11.7	6.5
100.0	663.3	36.5	19.7	17.1	8.3

Cavity volume, the difference between the densities of the gauge and shoulder sections of the same tensile specimen, was obtained after deformation, by weighing in air and in ethyl iodide.

Tensile tests were done in air by using an MTS universal testing machine. The tensile specimens of all five alloys were deformed by the differential strain-rate test technique from $\dot{\varepsilon} \sim 4 \times 10^{-6}$ to $3 \times 10^{-2} s^{-1}$ in order to study the effect of test temperature, grain size and alloy composition on the σ–$\dot{\varepsilon}$ relationship. Test temperatures were controlled to an accuracy of $\pm 1°$ C. A heating and soaking time of 1 h was given for each specimen prior to straining.

3. Results

Annealing of the tensile specimens for various lengths of time at 535° C produced different grain sizes as shown in Table II. The microstructures of the Al–Cu alloys of all the compositions investigated were presented earlier [19]. The respective phase sizes (p_κ and P_θ) are given in Table III.

The mean free path between the θ phase particles, Λ, was calculated from the size of θ phase, p_θ, and its volume fraction, f, according to the following relation [20–22]

$$\Lambda = \frac{2}{3}\frac{p_\theta}{f}(1-f) \tag{3}$$

The volume fractions of θ phase at the test temperature of 535° C were estimated from the Al–Cu equilibrium diagram. The values of Λ, determined as above, are given in Table IV. Λ is seen to decrease with the increase in copper content in the Al–Cu alloys. The deformation behaviour of the specimens, having the above specified values of microstructural parameters, is described below.

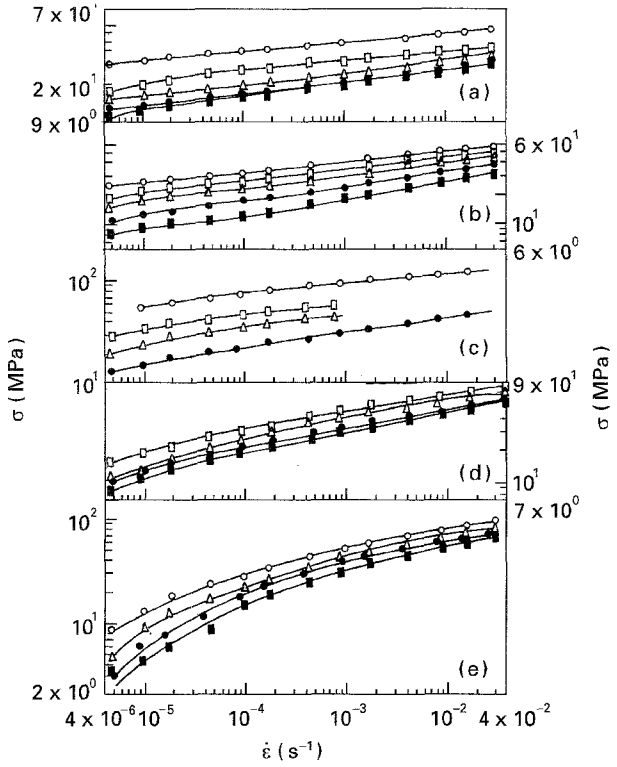

Figure 1 σ versus ε̇ plots at (○) 460, (□) 480, (△) 500, (●) 520 and (■) 535° C for the five Al–Cu alloys annealed for 0.5 h at 535° C: (a) Al–6Cu, (b) Al–11Cu, (c) Al–17Cu, (d) Al–24Cu and (e) Al–33Cu.

3.1. Effect of temperature

The tensile specimens annealed for 0.5 h at 535° C were deformed by the differential strain-rate test technique at four or five test temperatures individually in the range 460–535° C. The σ–ε̇ data were plotted on a log–log basis for all the alloys, as presented in Fig. 1.

The log σ–logε̇ plots of the Al–6Cu alloy show slopes, m, of ~0.10 at 460–500° C over the entire range of strain rates investigated. At 535° C, however, m increases to 0.18 over most of the strain-rate range and to 0.27 at very low strain rates. Similar behaviour is noticed for the Al–11Cu alloy also. The log σ–logε̇ curves of the alloys containing 17% or more copper exhibit two regions, with small m at higher strain rates (Region III) and large m at lower strain rates (Region II). Such a behaviour is apparent in the case of Al–33Cu alloy, Fig. 1e. In Region III, the average m increases marginally as the copper content increases from 6% to 33%. On the basis of m values, the alloys can be divided into two groups. For the Al–6Cu, Al–11Cu and Al–17Cu alloys the average m is 0.14, whereas for the other two alloys it is 0.19. Similarly, m increases from 0.28 for the Al–17Cu alloy to 0.55 for the Al–33Cu alloy at lower strain rates.

The activation energies for deformation, Q, in Regions II and III were determined at constant stresses according to the equation

$$Q = -R\left[\frac{\partial(\ln \dot{\varepsilon} T E^{n-1})}{\partial(1/T)}\right]_{\sigma,d} \quad (4)$$

The values of E for the Al–Cu alloys of different compositions were estimated from that of pure copper and pure aluminium at selected temperatures [23], employing the rule of mixture on the basis of atomic compositions. The average of n values at different temperatures involved was considered in each region. The Arrhenius plots, together with the values of Q, in Regions II and III for the different alloys are given in Figs 2 and 3, respectively. In view of the wide variations in the values of $\dot{\varepsilon}TE^{n-1}$, the different scales have been assigned along the ordinate for different alloys. The mean values of Q for the Al–24Cu and Al–33Cu alloys are found to be 171.5 kJ mol^{-1} in Region II and 211.0 kJ mol^{-1} in Region III. The alloys containing less copper, however, show much higher values of Q in Region III. The average value of

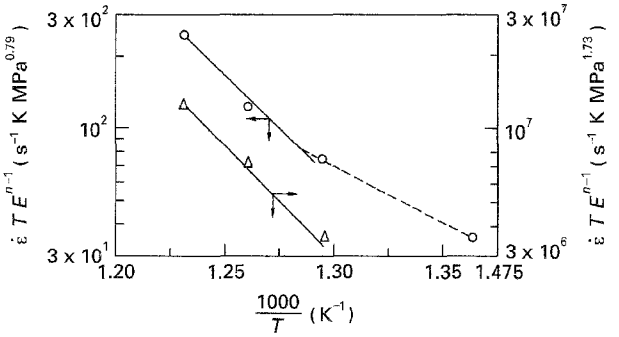

Figure 2 Arrhenius plots for determining the activation energy for superplastic deformation in the (△) Al–24Cu and (○) Al–33Cu alloys. (△) σ = 20 MPa, Q = 176.7 ± 12.8 kJ mol^{-1}; (○) σ = 10 MPa, Q = 166.2 ± 16.9 kJ mol^{-1} (≥ 778 K), Q = 87.7 kJ mol^{-1} (≤ 778 K).

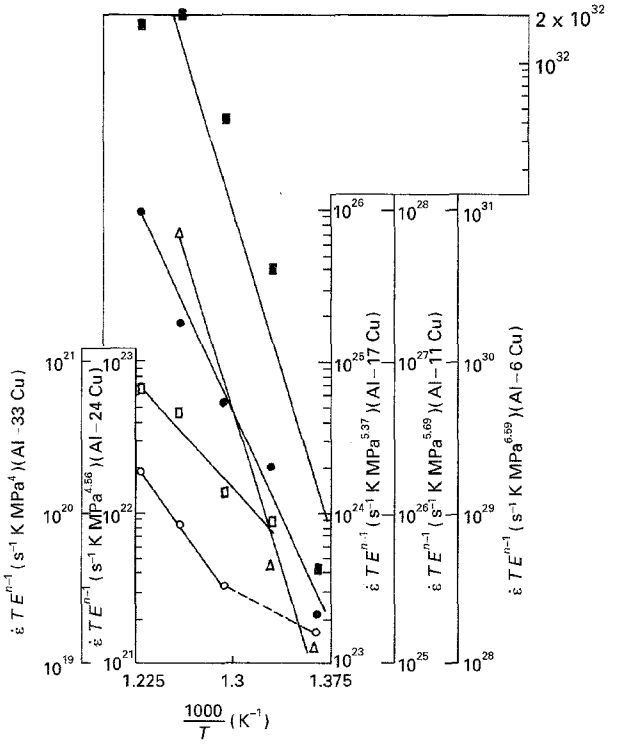

Figure 3 Arrhenius plots for determining the activation energy for deformation in Region III. (■) Al–6Cu, σ = 30 MPa, Q = 546.7 ± 107.1 kJ mol^{-1}. (●) Al–11Cu, σ = 30 MPa, Q = 373.4 ± 32.0 kJ mol^{-1}. (△) Al–17Cu, σ = 30 MPa, Q = 521.9 ± 87.9 kJ mol^{-1}. (□) Al–24Cu, σ = 52 MPa, Q = 184.0 ± 31.9 kJ mol^{-1}. (○) Al–33Cu, σ = 60 MPa, Q = 238.0 ± 5.9 kJ mol^{-1} (≥ 778 K), Q = 84.7 kJ mol^{-1} (≤ 778 K).

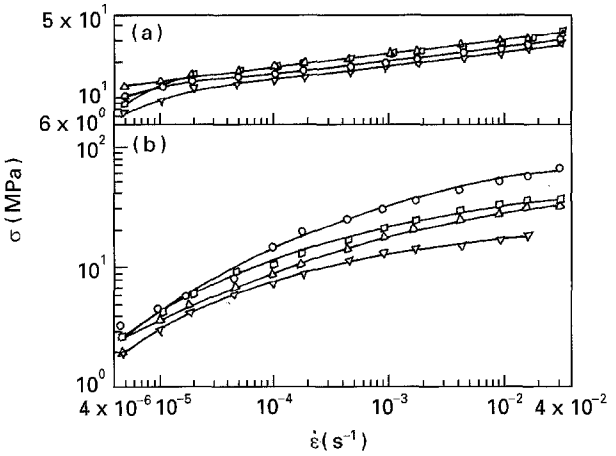

Figure 4 σ versus ε̇ plots at 535° C for (a) Al–6Cu and (b) Al–33Cu alloys of various grain sizes. (a) d_k (μm)/d_θ (μm): (○) 34.1/3.1; (□) 37.7/3.3; (△) 41.9/4.3; (▽) 55.3/4.0. (b) d_k (μm)/d_θ (μm): (○) 7.4/6.4; (□) 6.9/6.6; (△) 7.3/9.9; (▽) 9.3/8.8.

TABLE V Values of p in Regions II and III using various types of d

Region	Alloys	p based on			
		d_κ	d_θ	p_κ	p_θ
II	Al–24Cu	− 0.40	− 0.97	− 0.52	− 0.96
	Al–33Cu	− 2.83	− 2.55	− 1.49	− 2.44
III	Al–6Cu	− 2.04	0.33	− 0.48	6.10
	Al–11Cu	1.20	3.53	1.40	6.67
	Al–17Cu	0.66	0.48	2.78	0.02
	Al–24Cu	− 0.03	− 0.20	0.21	− 0.07
	Al–33Cu	− 12.0	− 13.20	− 7.80	− 13.80

Q for the Al–6Cu, Al–11Cu and Al–17Cu alloys is determined to be 480.7 kJ mol^{-1}. In the case of Al–33Cu alloy, however, Q appears to decrease to ~86 kJ mol^{-1} below a critical temperature of 778 K, Figs 2 and 3.

3.2. Effect of grain size

The tensile specimens of various grain sizes in all five alloys, Table II, were deformed to obtain σ–ε̇ data at 535 °C. The σ–ε̇ data were plotted for each alloy separately in order to examine the effect of grain size. Except for the Al–33Cu alloy, the log σ–log ε̇ curves, corresponding to different grain sizes, were found to lie within a narrow band of flow stresses, with no systematic effect of grain size. This is illustrated by the logσ–logε̇ curves for the Al–6Cu and Al–33Cu alloys in Fig. 4.

An attempt was made to determine p according to the equation

$$p = n\left[\frac{\partial \ln \sigma}{\partial \ln d}\right]_{\dot{\varepsilon},T} \quad (5)$$

in which d_θ, d_κ, p_θ, and p_κ, the grain size of θ phase, grain size of κ phase, phase size of θ phase and phase size of κ phase, respectively, were taken separately as d. In each region, the mean of n values, corresponding to the grain sizes involved, was taken. The values of

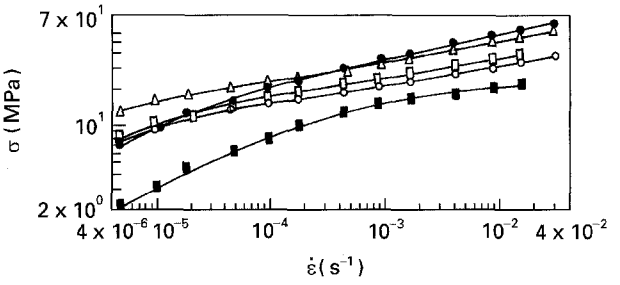

Figure 5 σ versus ε̇ plots at 535° C for the Al–Cu alloys of different compositions and annealed for 100 h at 535° C. (○) Al–6Cu, (□) Al–11Cu, (△) Al–17Cu, (●) Al–24Cu, (■) Al–33Cu.

p are given in Table V. Surprisingly, as seen in Fig. 4b, the flow stress increases with a decrease in grain size, which yields the negative values of p in some cases. Further, the effect of grain size in the Al–33Cu alloy is more pronounced in Region III than in Region II.

3.3. Effect of composition

The σ–ε̇ data for the various compositions, but annealed for the same time, were replotted together to examine the effect of composition at 535° C. For example, Fig. 5 shows such plots from the specimens annealed for 100 h. Four sets of such plots for the annealing times of 0.5, 4, 10 and 100 h were compared. The log σ–log ε̇ curves do not show any systematic effect of composition. The flow stresses at $\dot{\varepsilon} = 1 \times 10^{-5}$ and $1 \times 10^{-2}\,s^{-1}$, for the various compositions and annealing times, are given in Table VI.

The composition of the alloy affects both the phase proportion as well as the grain size. In view of a wide variation in p, Table V, and the absence of any systematic effect of composition on flow stress, Table VI, an attempt was made to examine if Λ, the mean free path, plays any role. The flow stresses at $\dot{\varepsilon} = 1 \times 10^{-6}$ and $1 \times 10^{-2}\,s^{-1}$ were plotted as a function of Λ on a log–log graph, Fig. 6, for all the alloy compositions and annealing times.

In Fig. 6, Λ decreases towards the left with increasing copper content. The data towards the largest value of Λ correspond to the Al–6Cu alloy, whereas that towards the smallest value of Λ correspond to the Al–33Cu alloy. At each strain rate, the four data points for each composition correspond to the four annealing times employed. The regression analysis of the data, Table VII, and Fig. 6, suggest linear relationships between logσ and logΛ, i.e.

$$\sigma = K\Lambda^B \quad (6)$$

where the proportionality constant, K, is represented by the intercept (log K) of log σ versus log Λ plot. The values of B and K are listed in Table VII.

From Fig. 7 and Table VII, the negligibly small B and very poor r values for the Al–17Cu and Al–24Cu alloys suggest a transitional behaviour between the positive and negative dependencies of σ on Λ. However, if the data of Al–17Cu, Al–24Cu and Al–33Cu alloys are combined together (solid lines at extreme left) then the relationship between σ and Λ, especially, at $\dot{\varepsilon} = 1 \times 10^{-5}\,s^{-1}$ can be approximately

TABLE VI Flow stresses at $\dot{\varepsilon}_1 = 1 \times 10^{-5}\,s^{-1}$ and $\dot{\varepsilon}_2 = 1 \times 10^{-2}\,s^{-1}$ at 535° C in the Al–Cu alloys of various compositions and annealed at 535° C for 0.5–100 h

Annealing time (h)	Flow stress (MPa) Al–6Cu		Al–11Cu		Al–17Cu		Al–24Cu		Al–33Cu	
	$\dot{\varepsilon}_1$	$\dot{\varepsilon}_2$	$\dot{\varepsilon}_1$	$\dot{\varepsilon}_2$	$\dot{\varepsilon}_1$	$\dot{\varepsilon}_2$	$\dot{\varepsilon}_1$	$\dot{\varepsilon}_2$	$\dot{\varepsilon}_1$	$\dot{\varepsilon}_2$
0.5	13.0	28.5	9.5	25.4	16.0	43.0	11.0	51.5	4.7	53.5
4.0	12.6	33.0	11.3	33.0	14.3	46.0	9.3	50.0	4.6	33.5
10.0	14.2	32.0	10.2	29.0	12.5	42.0	8.5	43.0	3.9	30.0
100.0	9.4	26.5	10.5	30.0	16.0	43.0	9.4	48.0	3.0	17.6

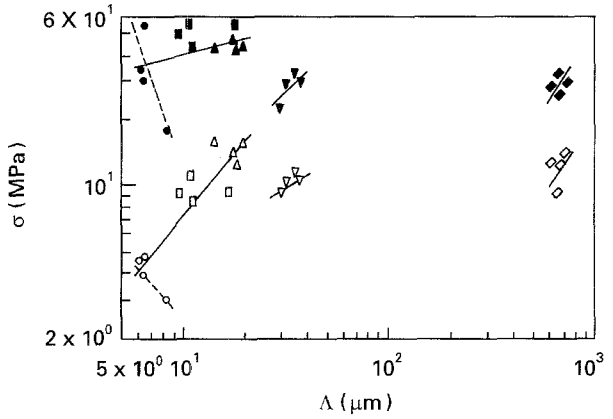

Figure 6 Dependence of flow stress, σ, on mean free path, Λ, at $\dot{\varepsilon}$ = (◇, ▽, △, □, ○) 1×10^{-5} and (◆, ▼, ▲, ■, ●) $1 \times 10^{-2}\,s^{-1}$, at 535° C. (◇, ◆) Al–6Cu, (▽, ▼) Al–11Cu, (△, ▲) Al–17Cu, (□, ■) Al–24Cu, (○, ●) Al–33Cu.

given by

$$\sigma = 0.5\,\Lambda^{1.16} \qquad r = 0.86 \tag{6}$$

To summarize, the σ–$\dot{\varepsilon}$ relationship for the Al–Cu alloys containing 6%–33% Cu can be given by

$$\sigma \propto \dot{\varepsilon}^m \Lambda^B \exp(Q/RT) \tag{7}$$

where the values of m, B and Q depend on alloy composition and strain-rate regime.

3.4. Microstructural evolution

In order to follow the microstructural evolution during deformation, some tensile specimens were deformed at constant initial strain rates to the selected strain levels. There occurred enhanced grain growth and cavitation in the gauge section as compared to the shoulder section of the same tensile specimen. However, some specimens having initially coarse grains exhibited a decrease in grain size on deformation. Listed in Table VIII are the values of grain size and cavity volume at selected test conditions.

4. Discussion

The Al–Cu alloys of different compositions deformed over the strain-rate range $\sim 4 \times 10^{-6}$ to $3 \times 10^{-2}\,s^{-1}$ and the temperature range 460–535° C exhibit, predominantly, Region III behaviour and limited Region II behaviour. Superplastic behaviour with $m \geq 0.3$ appears as the test temperature or the amount of copper in the alloy is increased.

For structural superplasticity the grain size should be $\leq 10\,\mu m$. While the grain sizes of θ phase in all the alloys, Table II, satisfy this criterion, the grain sizes of κ phase are larger in the Al–6Cu and Al–11Cu alloys. However, it should be noted that, although the grain sizes of both the phases are generally greater than 10 μm in the Al–17Cu, Al–24Cu and Al–33Cu alloys, superplastic behaviour, m, is more pronounced in the Al–33Cu alloy only, Fig. 1. The difference in the extent of superplasticity, between Al–24Cu and Al–33Cu alloys, is noted in spite of the comparable values of the grain sizes (Table II, annealing time = 0.5 h).. Thus, the grain size does not seem to be a critical criterion for the observed difference in the flow behaviour of the two alloys. Instead, Λ is found to be less than 10 μm in the Al–33Cu alloy only, whereas it is $\geq 10\,\mu m$ in all other alloys (e.g. see Table IV). Therefore, Λ may be a more appropriate parameter than the grain size for relating to superplastic behaviour.

In the superplastic region, the value of p in Equation 1 is known [2] to be 2–3 whereas $p = 0$ in Region III. In the Al–Cu eutectic alloy, $p = 2$ has been reported [5] in Region II. The present values of p, Table V, on the other hand, are mostly found to be negative with a wide variation in the magnitudes which may be contributed by the following possibilities.

TABLE VII Values of K and B in the relation $\sigma = K\Lambda^B$ for the various alloy compositions at two strain rates (r = regression coefficient of log σ versus log Λ plot)

Alloy	$\dot{\varepsilon} = 1 \times 10^{-5}\,s^{-1}$			$\dot{\varepsilon} = 1 \times 10^{-2}\,s^{-1}$		
	K	B	r	K	B	r
Al–6Cu	1.5×10^{-3}	1.38	0.39	2×10^{-3}	1.44	0.72
Al–11Cu	1.19	0.62	0.80	1.07	0.95	0.82
Al–17Cu	36.77	−0.32	0.35	46.19	−0.02	0.07
Al–24Cu	10.49	−0.04	0.09	61.39	−0.09	0.21
Al–33Cu	71.05	−1.49	0.91	6.83×10^{3}	−2.79	0.77

TABLE VIII Grain sizes (d_0 = initial grain size, d = final grain size) and cavity volume, C_v, upon deformation under various test conditions

Alloy	d_0 (μm)	$\dot{\varepsilon}$ (s^{-1})	T (°C)	ε(%)	d(μm)	C_v(%)
Al–24Cu	7.6	1.1×10^{-3}	460	12	7.9	12.3
			460	31	8.9	15.4
			540	12	8.5	12.2
		2×10^{-5}	540	25	8.7	12.8
	21.0	2×10^{-5}	540	12	12.8	11.5
Al–6Cu	30.8	1.1×10^{-3}	540	12	72.4	6.8

During high-temperature deformation of the Al–Cu alloys there occur grain growth and cavitation, Table VIII, with the former causing an increase [8] and the latter a decrease [13] in flow stress. If the grain growth is more predominant in the case of fine grains but the cavitation is more predominant in the case of coarse grains, as reported in the literature [5, 24], the strength of the samples having the fine microstructure should exceed, at some strain, the strength of that having initially coarse microstructure. Such may be a reason for the wide variation in the magnitude of p found here. Also, in a recent study on the flow behaviour of the separate θ phase, Chanda and Murty [25] noted the validity of the Hall–Petch [26, 27]-type relationship up to 575° C, showing an increase in flow stress with the decrease in grain size. During the co-existence of κ and θ phases in the alloys used in the present work, the deformation behaviour is significantly influenced by the presence of θ phase; in which case p may deviate from that known conventionally for the high-temperature deformation [2].

With increase in the copper content, the proportion of the θ phase in the Al–Cu alloy increases. This increase may contribute to the rise in flow stress due to the inherently harder nature of the θ phase. In the Al–Cu alloys containing 3%–5% Cu, the strength has been shown [28] to increase in the proportion of f/d_θ value. However, in the present study, the data with scatter, Table VI and Fig. 6 (Region III), generally suggest that the flow stress first increases then decreases as the volume fraction of the θ phase and f/d_θ are increased. Such composition-dependent variation in flow stress was attributed [29] to a change in the deformation mechanism and the difference in the concurrent microstructural evolution. From the analysis of several results on the variation in strength as a function of volume fraction of the second-phase particles, Movchan [30] has suggested that the strength should increase up to about 66 vol % of the stronger second-phase particles, then a decrease is expected. At this proportion the particles delay the movement of dislocations in the matrix with a similar efficiency in all directions, saturating the strengthening capability of the second phase.

Between Al–6Cu and Al–11Cu alloys, σ may be said to be approximately independent of Λ but, within each of these, σ increases with Λ, Fig. 7. This trend is opposite to the effect of Λ on yield strength, tensile strength and hardness of several two-phase materials [30] at low temperatures. The difference in the relations between σ and Λ at low temperature compared with high temperatures, is similar to the change from the Hall–Petch-type relationship [26, 27] between the grain size and flow stress at low temperatures to the high-temperature relationship, given in Equation 1.

During high-temperature deformation itself, in some cases, σ increases with Λ whereas, in other cases, they are inversely related, Fig. 7 and Table VII. During deformation of fine-grained materials, grain-boundary sliding (GBS) is accompanied, to different extents, by diffusional creep at lower strain rates and by intragranular slip at higher strain rates. The principal equation for slip can be written as [31]

$$\dot{\varepsilon}_{\text{slip}} = A_s\left[\frac{\Lambda}{b}\right]^3\left[\frac{D_L}{b^2}\right]\left[\frac{\sigma}{E}\right]^8 \tag{8}$$

where A_s is a constant, D_L is the lattice diffusion coefficient and Λ is the minimum barrier spacing governing slip creep (typically the interparticle spacing). Equation 8 gives an inverse relation between σ and Λ ($B = -0.38$, according to Equation 6), which may account for some of the negative values of B in Table VII. Although more data are needed in view of the large scatter, two tentative explanations are provided below for the observed relations between σ and Λ.

(i) In the Al–6Cu and Al–11Cu alloys, the non-deformable θ phase, distributed as discrete particles [19], may act as sites for cavity nucleation when the stress concentration, built up by deformation of the surrounding softer matrix, reaches a high value. Then, as Λ increases the cavity spacing increases or the cavity density decreases. In addition, a larger proportion of the matrix, in this case, may undergo work hardening before the stress concentration is relieved by cavity nucleation. Therefore, a higher flow stress for the larger value of Λ may be expected in these alloys. In the alloys containing a higher amount of copper, e.g. Al–33Cu alloy, the contiguous κ and θ grains are formed with longer interphase interface along which sliding may occur. During superplastic deformation of the Al–Cu eutectic alloy, grain-boundary sliding contributes ~70% of the total strain [32]. For smaller Λ the proportion of the interphase boundary increases and, probably, the contribution of grain-boundary sliding is enhanced because its accommodation by diffusional or intragranular slip becomes easier. On the other hand, the ability to accommodate grain-boundary sliding is reduced when Λ becomes larger. Thus, the amount of cavities may increase with Λ, leading to a lower flow stress. Therefore, in the alloys, which have both the κ and θ phases present as distinct grains, σ decreases with the increase in Λ.

(ii) In particle-containing systems, as is the Al–Cu alloy, especially, for lower copper contents, competition occurs between cutting and bowing processes [33] during deformation. With increasing particle size, therefore, the flow stress first increases due to cutting then decreases due to bowing for a fixed volume fraction of second phase. As the volume fraction is increased, the transition from cutting to bowing occurs at smaller particle size. With the increase in copper content, the proportion of θ phase increases and so

also does its average size. Accordingly, the dominance of cutting is expected in the lower copper content alloys and so the flow stress can increase with copper level. For higher copper contents, the dominance of the bowing process can be responsible for the observed decrease in flow stress as seen in Fig. 5. Thus, through the effect of size and volume fraction of particles on the stress required for cutting and bowing, the dependence of σ on Λ can also change from a positive to negative value of B with increasing copper content, as listed in Table VII.

The value of $m = 0.55$ for the Al–33Cu alloy is typical of the superplastic behaviour ($m = 0.5$). The slightly lower values of m in other compositions may be due to the inadequately developed Region II. The activation energy for deformation in Region II, at higher temperatures (171.5 kJ mol^{-1}), is comparable with the activation energy for the deformation of the Al–Cu eutectic (167 kJ mol^{-1}) [5] and Al–17Cu (163 kJ mol^{-1}) [16] alloys reported earlier. It is interesting to note that the activation energy of the κ-matrix has been reported [18] to be 156 kJ mol^{-1}, whereas that of the θ phase is 213 kJ mol^{-1}, based on the hot hardness data. These values amply compare with the activation energy for the deformation of the Al–24Cu and Al–33Cu alloys in Regions II and III, respectively. However, the activation energy of 86 kJ mol^{-1} in Region II, for the Al–33Cu alloy, below the critical temperature of 773 K, is closer to the activation energy for the κ–θ interphase boundary diffusion (97 kJ mol^{-1}) [34]. Thus, while the m values are in agreement with the predictions of several theories [31], according to which superplastic deformation occurs by grain-boundary sliding, the larger values of Q seem to suggest the importance of lattice diffusion as the accommodation process.

The values of m ($\sim$0.1–0.2) in Region III are comparable with that for other superplastic and non-superplastic materials. A small difference in m between the two groups of compositions may have some significance, in conformity with the difference in the Q values. Thus, for the Al–24Cu and Al–33Cu alloys $n \sim 5$ and $Q = 211$ kJ mol^{-1}, whereas $n \sim 7$ and $Q = 480.7$ kJ mol^{-1}, for the Al–6Cu, Al–11Cu alloys, are considered here. As the former value of Q is in agreement with the activation energy of the θ phase, as well as for lattice diffusion in pure copper (211 kJ mol^{-1}) [35], the deformation in Region III is suggested to occur by a dislocation climb mechanism [36].

The values of Q for the Al–6Cu, Al–11Cu and Al–17Cu alloys (480.7 kJ mol^{-1}) is much higher than the activation energy for lattice diffusion. Such a high value of Q in the precipitation- and dispersion-strengthened alloys is explained by using the concept of internal or back stress [36]. Furushiro and Hori [11] reported an increase in the ratio of internal stress, σ_i, to applied stress, σ, i.e. σ_i/σ, with the decrease in the copper content in the Al–Cu alloys. From their data of applied stress and effective stress, the value of activation energy, based on effective stress σ_e ($\sigma_e = \sigma - \sigma_i$) at two temperatures, was estimated to be only half of that based on σ at $\dot{\varepsilon} = 5 \times 10^{-3}$ s^{-1}. Also, the dispersion of hard second-phase particles may enhance the probability of cell/subgrain formation which, in turn, can account for the slightly higher value of n (7) in this region. The substitution of the relationship between substructure size and stress [37], namely $\sigma \propto$ (cell size)$^{-1}$ or $\sigma \propto$ (subgrain size)$^{-0.5}$, in the creep equation was proposed by Sherby *et al.* [38] to reduce the value of n to 4 and 5.5 for the cell and subgrain structures, respectively. Therefore, in this group of alloys also, the deformation in Region III is suggested to occur by dislocation climb.

5. Conclusions

The stress–strain rate (σ–$\dot{\varepsilon}$) data of the Al–6Cu, Al–11Cu, Al–17Cu, Al–24Cu and Al–33Cu alloys, over $\dot{\varepsilon} \sim 4 \times 10^{-6}$ to 3×10^{-2} s^{-1} and $T =$ 460–535° C, lead to the following conclusions.

1. The Al–33Cu alloy shows superplastic behaviour over an order of strain rates. In other compositions, such a behaviour is noticeable marginally at $\dot{\varepsilon} \leq 1 \times 10^{-5}$ s^{-1}, especially, towards higher temperatures. For superplastic deformation, the strain-rate sensitivity index, m, and activation energy, Q, are estimated to be $\sim$0.5 and 171.5 kJ mol^{-1}, respectively.
2. The Al–Cu alloys can be divided into two groups on the basis of stress exponent ($n = 1/m$) and Q values in Region III. For the group I alloys, including Al–6Cu, Al–11Cu and Al–17Cu compositions, $n \sim 7$ and $Q = 480.7$ kJ mol^{-1}, whereas for the group II alloys, including Al–24Cu and Al–33Cu compositions, $n \sim 5$ and $Q = 179$ kJ mol^{-1} have been obtained. Deformation in Region III is suggested to be controlled by dislocation climb in all the alloys, provided the concept of back stress is introduced to reduce the higher value of Q for the first group.
3. Superplastic behaviour cannot be satisfactorily related to the fine grain or phase size. Instead, the mean free path between the θ phases appears to be a better criterion for superplasticity which, from the present results, requires that Λ should be less than 10 μm.
4. Flow stress increases with Λ in the Al–6Cu and Al–11Cu alloys, whereas they are inversely related in the Al–33Cu alloy. Such dependencies are explained through the influence of Λ and the nature of the phase distribution on the cavitation behaviour of these alloys. Alternatively, the dominance of dislocation cutting process in the lower copper content alloys, and the dominance of dislocation bowing process in the higher copper content alloys can lead to such dependencies of stress on Λ.

References

1. A. K. MUKHERJEE, J. E. BIRD and J. E. DORN, *Trans. ASM* **62** (1969) 155.
2. J. W. EDINGTON, K. N. MELTON and C. P. CUTLER, *Prog. Mater. Sci.* **21** (1976) 61.
3. M. SUÉRY and B. BAUDELET, *Res. Mech.* **2** (1981) 163.
4. M. KOBAYASHI and M. MIYAGAWA, *Trans. ISIJ* **27** (1987) 685.
5. D. L. HOLT and W. A. BACKOFEN, *Trans. ASM* **59** (1966) 755.

6. M. J. STOWELL, J. L. ROBERTSON and B. M. WATTS, *Metal Sci. J.* **3** (1969) 41.
7. R. D. SCHMIDT-WHITLEY, *Z. Metallkd* **64** (1973) 552.
8. G. RAI and N. J. GRANT, *Metall. Trans.* **6A** (1975) 385.
9. K. A. PADMANABHAN and G. J. DAVIES, *Metal Sci.* **11** (1977) 177.
10. Y. KOBAYASHI, Y. ISHIDA and M. KATO, *Scripta Metall.* **11** (1977) 51.
11. N. FURUSHIRO and S. HORI, *ibid.* **12** (1978) 35.
12. G. A. NASSEF, M. SUERY and EL-ASHRAM, *Metals Techno.* **9** (1982) 355.
13. B. P. KASHYAP and K. TANGRI, *Metall. Trans.* **181A** (1987) 417.
14. E. SATO, K. KURIBAYASHI and R. HORIUCHI, *J. Jpn Inst. Metals* **53** (1989) 885.
15. A. H. CHOKSHI and T. G. LANGDON, *Mater. Sci. Technol.* **5** (1989) 435.
16. J. R. CAHOON, *Metal Sci.* **9** (1975) 346.
17. P. K. CHAUDHURY and F. A. MOHAMED, *Mater. Sci. Eng. A* **101** (1988) 13.
18. G. S. SOHAL, *Mater. Sci. Technol.* **4** (1988) 811.
19. P. K. BAKSHI and B. P. KASHYAP, *J. Mater. Sci.* **29** (1994) 2063.
20. B. I. EDELSON and W. M. BALDWIN, *Trans. ASM* **55** (1962) 230.
21. M. F. ASHBY, *Z. Metallkd* **55** (1964) 5.
22. C. W. CORTI, P. COTTERILL and G. A. FITZPATRICK, *Int. Metall. Rev.* **19** (1974) 77.
23. A. G. GUY, "Elements of physical metallurgy," 2nd Edn. (Addison-Wesley, Reading, MA, 1959) p. 297.
24. D. W. LIVESEY and N. RIDLEY, *J. Mater. Sci.* **27** (1982) 2257.
25. T. CHANDA and G. S. MURTY, *ibid.* **27** (1992) 5931.
26. E. O. HALL, *Proc. Phys. Soc., Lond.* **B64** (1951) 747.
27. N. J. PETCH, *J. Iron Steel Inst.* **174** (1953) 25.
28. D. DEW-HUGHES and W. D. ROBERTSON, *Acta Metall.* **8** (1960) 147.
29. P. K. BAKSHI and B. P. KASHYAP, *Scripta Metall. Mater.* **29** (1993) 1073.
30. B. A. MOVCHAN, *Mater. Sci. Eng.* **A138** (1991) 109.
31. O. D. SHERBY and J. WADSWORTH, *Prog. Mater. Sci.* **33** (1989) 169.
32. S. HORI, N. FURUSHIRO and S. KAWAGUCHI, *J. Jpn Inst. Light Metals* **25** (1975) 361.
33. T. H. COURTNEY, "Mechanical behaviour of materials", (McGraw-Hill, Singapore, 1990) p. 193.
34. E. HO and G. C. WEATHERLY, *Acta Metall.* **23** (1975) 1451.
35. E. A. BRANDES (ed.), "Smithells metals reference book", 6th Edn (Butterworths, London, 1983) p 13.9.
36. J. CADEK, "Creep in metallic materials", 1st Edn. (Elsevier, Amsterdam, 1988) pp. 115, 176.
37. A. W. THOMPSON, *Metall. Trans.* **8A** (1977) 833.
38. O. D. SHERBY, R. H. KLUNDT and A. K. MILLER, *ibid.* **8A** (1977) 843.

Received 22 December 1994
and accepted 2 May 1995